

# Optical properties of human normal small intestine tissue determined by Kubelka-Munk method *in vitro*

Hua-Jiang Wei, Da Xing, Guo-Yong Wu, Ying Jin, Huai-Min Gu

**Hua-Jiang Wei, Da Xing, Ying Jin, Huai-Min Gu**, Institute of Laser Life Science, South China Normal University, Guangzhou, 510631, Guangdong Province, China

**Hua-Jiang Wei**, Department of Physics, Guangdong College of Pharmacy, Guangzhou, 510224, Guangdong Province, China

**Guo-Yong Wu**, Department of Surgery, the First Affiliated Hospital, Sun Yat-Sen Medical University, Guangzhou, 510080, Guangdong Province, China

**Supported by** the Special Funds of National Key Basic Research Project of China, No. 2002CCC0 0400 and the Team Project of Natural Science Foundation of Guangdong Province, No.015012

**Correspondence to:** Da Xing, Institute of Laser Life Science, South China Normal University, Shipai, Tianhe District, Guangzhou 510631, Guangdong Province, China. xingda@hsut.scnu.edu.cn

**Telephone:** +86-20-85210089 **Fax:** +86-20-85216052

**Received:** 2002-12-22 **Accepted:** 2003-03-26

## Abstract

**AIM:** To study the optical properties of human normal small intestine tissue at 476.5 nm, 488 nm, 496.5 nm, 514.5 nm, 532 nm, 808 nm wavelengths of laser irradiation.

**METHODS:** A double-integrating-sphere system, the basic principle of measuring technology of light radiation, and an optical model of biological tissues were used in the study.

**RESULTS:** The results of measurement showed that there were no significant differences in the absorption coefficients of human normal small intestine tissue at 476.5 nm, 488 nm, 496.5 nm laser in the Kubelka-Munk two-flux model ( $P>0.05$ ). The absorption coefficients of the tissue at 514.5 nm, 532 nm, 808 nm laser irradiation were obviously increased with the decrease of these wavelengths. The scattering coefficients of the tissue at 476.5 nm, 488 nm, 496.5 nm laser irradiation were increased with the decrease of these wavelengths. The scattering coefficients at 496.5 nm, 514.5 nm, 532 nm laser irradiation were obviously increased with the increase of these wavelengths. The scattering coefficient of the tissue at 532 nm laser irradiation was bigger than that at 808 nm. There were no significant differences in the total attenuation coefficient of the tissue at 476.5 nm and 488 nm laser irradiation ( $P>0.05$ ). The total attenuation coefficient of the tissue at 488 nm, 496.5 nm, 514.5 nm, 532 nm, 808 nm laser irradiation was obviously increased with the decrease of these wavelengths, and their effective attenuation coefficient revealed the same trend. There were no significant differences among the forward scattered photon flux, backward scattered photon flux, and total scattered photon flux of the tissue at 476.5 nm, 488 nm, 496.5 nm laser irradiation. They were all obviously increased with attenuation of tissue thickness. The attenuations of forward and backward scattered photon fluxes, and the total scattered photon flux of the tissue at 514.5 nm laser irradiation were slower than those at 476.5 nm, 488 nm, 496.5 nm laser irradiation respectively. The attenuations of forward and backward scattered photon fluxes, and total scattered photon fluxes at 532 nm laser irradiation were obviously slower

than those at 476.5 nm, 488 nm, 496.5 nm, 514.5 nm laser irradiation. The attenuations of forward and backward scattered photon fluxes, and total scattered photon flux at 808 nm laser irradiation were all obviously slower than those at 476.5 nm, 488 nm, 496.5 nm, 514.5 nm, 532 nm laser irradiation respectively.

**CONCLUSION:** There are significant differences in optical parameters of human normal small intestine tissue in the Kubelka-Munk two-flux model at six different wavelengths of laser radiation. The results would provide a new method of information analysis for clinical diagnosis.

Wei HJ, Xing D, Wu GY, Jin Y, Gu HM. Optical properties of human normal small intestine tissue determined by Kubelka-Munk method *in vitro*. *World J Gastroenterol* 2003; 9(9): 2068-2072 <http://www.wjgnet.com/1007-9327/9/2068.asp>

## INTRODUCTION

Much effort is being made in the study of light propagation in tissues due to the development and wide use of lasers in surgery and therapy<sup>[1-3]</sup>. In particular, the effectiveness of photodynamic therapy (PDT) is greatly influenced by photosensitizer content and light distribution in the irradiated tissue<sup>[4-7]</sup>, and an accurate evaluation of energy fluence in depth should allow an estimate of whether the whole tumor mass is properly irradiated<sup>[8,9]</sup>. Consequently, determination of tissue optical properties is important. Photons are absorbed and scattered when they come into contact with biological tissues<sup>[10]</sup>. The depolarization degree of different biological tissues at linearly polarized light is different. All these have a correlation with the components and structures of biological tissues and optical properties. Consequently, photons have already taken the information that has a close relationship with the components and structures of biological tissues since photons came into contact with biological tissues<sup>[11-13]</sup>. Biological tissues may be looked upon as turbid media from the point of view of tissue optics. The optical properties of biological tissues change with the characteristics of living organisms<sup>[14-17]</sup>. The typical optical properties are obtained by using solutions of the radiative transport equation that expresses the optical properties in terms of readily measurable quantities. These solutions are either exact or approximate and correspond to the direct or indirect methods. A double-integrating-sphere system, the basic principle of measuring technology of light radiation, an optical model of biological tissues were used in this experiment<sup>[18-21]</sup>. In our study, we detected the optical properties of human normal small intestine tissue at 476.5 nm, 488 nm, 496.5 nm, 514.5 nm, 532 nm, 808 nm wavelengths of laser irradiation, and analyzed the experimental results.

## MATERIALS AND METHODS

The optical properties of tissues describe the three-dimensional propagation of radiation. Through modeling simplifications (i.e., Kubelka-Munk Two-Flux Theory) the radial propagation

is often reduced to a one-dimensional propagation of radiation. Kubelka-Munk two-flux theory was used to calculate the absorption coefficient  $A_{KM}$ , scattering coefficient  $S_{KM}$ , total attenuation coefficient  $E_t$  and effective attenuation coefficient  $E_{eff}$  of human normal small intestine tissue at six laser wavelengths by measuring reflection  $R$ , transmission  $T$  of diffuse irradiance on a slab of thickness  $d$  of the sample.

### Kubelka-Munk two-flux theory

The Kubelka-Munk two-flux theory is applied to the thin slab of scattering material without sources, and its prime advantage as compared to more complicated models is that the scattering coefficient  $S_{KM}$  and absorption coefficient  $A_{KM}$  can be directly expressed in terms of the measured reflection  $R$ , transmission  $T$ , and thickness  $d$  of the sample<sup>[22]</sup>. Consequently, it has been widely applied. Its parameters are commonly used in the field of medical physics. It regards the scattering light as none but the forward scattered photon fluxes  $i(x)$  and backward scattered photon fluxes  $j(x)$  when incident light radiates in a slab of thickness  $X$  (cm) of the turbid media. The sum of the forward and backward scattered photon fluxes is equal to the total scattered photon fluxes  $I(x)$ <sup>[23]</sup>. The scattering and absorption coefficients exist<sup>[24]</sup>. The description of  $A_{KM}$  and  $S_{KM}$  as a function of  $R$ ,  $T$ , and  $X$  are given by

$$A_{KM} = \left[ (1 + R^2 + T^2) / 2R - 1 \right] S_{KM} \quad (1)$$

$$S_{KM} = \frac{1}{Xb} \ln \left[ \frac{1 - R/(a+b)}{T} \right] \quad (2)$$

The description of total attenuation coefficients  $E_t$  and effective attenuation coefficients  $E_{eff}$  as a function of  $A_{KM}$  and  $S_{KM}$  are given by<sup>[25]</sup>

$$E_t = A_{KM} + S_{KM} \quad (3)$$

$$S_{KM} = \frac{1}{Xb} \ln \left[ \frac{1 - R/(a+b)}{T} \right] \quad (4)$$

The human normal small intestine tissue was regarded as a slab of turbid medium of thickness  $X$ . Then,  $A_{KM}$ ,  $S_{KM}$ ,  $E_t$ ,  $E_{eff}$  were respectively regarded as the absorption coefficients, scattering coefficients, total attenuation coefficients, effective attenuation coefficients of human normal small intestine tissue at laser irradiation.

### Materials

**Sample preparation** The sample used in our experiments was obtained within 2 hours after human normal small intestine tissue resection from one subject. The sample was rinsed briefly in saline to remove excess surface blood, and peeled off surface fats. The sample was cut with scissors along its direction of axis and stored at  $-70^\circ\text{C}$  until the experiments. For the thin tissues, two-faces of sample were not cut by microtome in order to keep integrity of the sample. Because the area of a slice of sample cut by microtome was large, the cytoplasmic liquid exuded severely, which increased the excessive liquid on the surface of the sample. Consequently, the measured results were influenced. The tissue-sample holder was designed and made from a black piece of opacity that was rounded with scissors. The piece was drilled two holes, and its inside radius and outside radius were respectively equal to 6 mm and 12 mm, as shown in Figure 1. The sample was spread out on the tissue-sample holder and nipped. The sample area and thickness were respectively  $16.1\text{ mm} \times 16.4\text{ mm}$  and  $1.42 \times 0.16\text{ mm}$ , and then it was put in the sample-pool of a double-integrating-sphere system to be measured. The whole experimental process took 4 hours, including sample preparation and taking the sample.

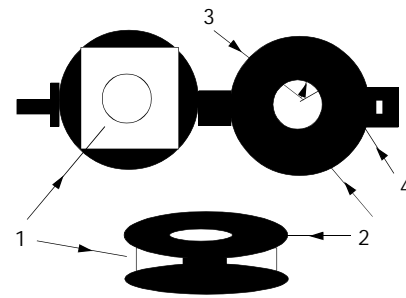


**Figure 1** Exhibition map of the tissue- sample holder. 1. Tissue-sample, 2. Tissue- sample holder, 3.  $R_a=6\text{ mm}$  4.  $R_b=12\text{ mm}$ .

### Methods

**Measurement of diffuse reflectance and transmittance** The double-integrating-sphere system was a traditional technique to obtain the diffuse reflectance and transmittance of a sample<sup>[26-28]</sup>. A double-integrating-sphere system shown in Figure 2 consisted of Ti: S ring laser (COHERENT, model 899-05), an argon ion laser (COHERENT, model: INNOVA 70), light attenuator, mirror, 2 mm pinhole, 6 mm pinhole, beam expander of 25 times, two integrating-spheres and two detectors and two optical traps (Anhui Institute of Optics and Fine Mechanics, Academia Sinica, China, model: F4). A Ti:S ring laser emitted at 532 nm and 808 nm wavelengths of laser. An argon ion laser emitted at 476.5 nm, 488 nm, 496.5 nm and 514.5 nm wavelengths of laser. The structures of the two integrating-spheres were the same, the diameter of the sphere was 0.05 m. The diameter of entrance and exit port of the integrating-spheres was equally 0.012 m. The laser beam was passed through two light attenuators, and reflected by the mirror. It was passed through a 2 mm pinhole, and expanded into a collimated laser beam by the beam expander of 25 times. It was passed through a 6 mm pinhole, and perpendicularly incident on the sample. The integrating-sphere I was only used to measure the diffuse reflectance  $R_d$  of the sample, not including the specularly reflected light of the sample. The optical trap backed of sample was used for light extinction, including the transmitted light and the diffusely transmitted light. The other optical trap backing the integrating-sphere II was used for light extinction, including all exiting light. The integrating-sphere II was only used to measure the diffuse Transmittance  $T_d$  of the sample, not including the collimatedly transmitted light. In this experiment, the diffuse reflectance and transmittance of the wall and the ectexine of the thin sample at 476.5 nm, 488 nm, 496.5 nm, 514.5 nm, 532 nm, 808 nm wavelengths of laser were measured.

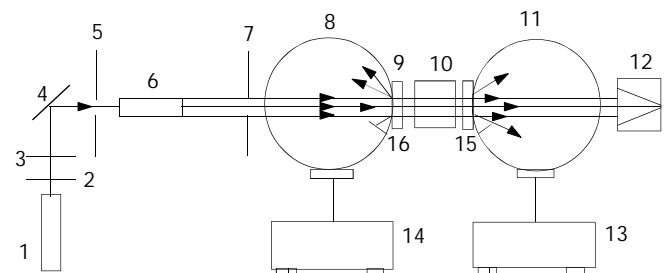


**Figure 2** A double-integrating-sphere system was used to determine the optical properties of biological tissues. 1. Laser, 2. Attenuator, 3. Attenuator, 4. Mirror, 5. 2 mm pinhole, 6. Beam expander, 7. 6 mm pinhole, 8. Intergrating sphere I, 9. Sample, 10. Optical trap, 11. Intergrating sphere II, 12. Optical trap, 13. Detector system, 14. Detector system, 15. Baffle, 16. Baffle.

The measuring method of diffuse reflectance was the same as reported<sup>[24]</sup>. The diffuse reflectance of the sample was given by

$$R_d = \left( \frac{K_s}{K_p} \right) r \tag{5}$$

where  $K_p$  is the diffuse reflection value of the standard target,  $K_s$  is the diffuse reflection value of the sample,  $\rho$  is the reflection coefficient of the standard target. The diffuse transmittance of the sample was given by

$$T_d = \frac{I_s}{I_0} \tag{6}$$

where  $I_s$  is the diffuse transmission value of the sample,  $I_0$  is the total transmission value. Figure 3 shows the arrangement to measure the total transmission value. The half-angle subtended by this aperture from the sample was  $3^\circ$ , and the standard target was placed at the exit port of integrating-sphere II. The wall and ekstexine of the sample were respectively radiated at laser and measured.

**Measurement of specular reflectance and collimated transmittance**

Figure 3 shows the arrangement and method to measure the specularly reflected light, collimated light and the total transmitted light. The half-angle subtended by this aperture from the sample was  $3^\circ$ , and the standard target was placed at the exit port of integrating-sphere II. The other was the same as Figure 2. The integrating-sphere I was used to measure the diffusely and specularly reflected light of the sample. The integrating-sphere II was used to measure the diffusely and collimatedly transmitted light of the sample, and the sum of the diffusely and collimatedly transmitted light of the sample was the totally transmitted light of the sample. The specular reflectance of the sample was given by

$$R_m = \left( \frac{K'_s}{K'_p} \right) r - R_d \tag{7}$$

where  $K'_p$  is the diffuse reflection value of the standard target,  $K'_s$  is the diffuse reflection value of the sample,  $R_d$  is the diffuse reflectance of the sample,  $R_m$  is the specular reflectance of the sample. The collimated transmittance of the sample was given by

$$T_c = \frac{I'_s}{I'_0} - T_d \tag{8}$$

where  $T_d$  is the diffuse transmittance of the sample,  $T_c$  is the collimated transmittance of the sample,  $I'_s$  is the diffuse transmission value of the sample,  $I'_0$  is the total transmission value.

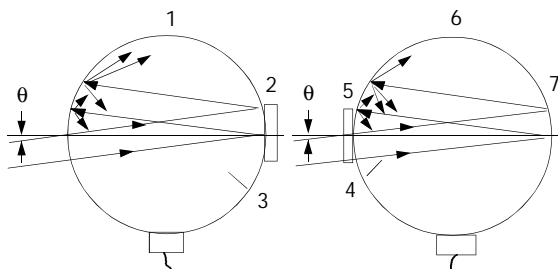


**Figure 3** Measuring set of specular reflectance and collimated transmittance of biological tissues. 1. Intergrating sphere I 2. Sample 3. Baffle 4. Baffle 5. Sample 6. Intergrating sphere II 7. Standard reference plate  $\theta=3^\circ$ .

**Statistical analysis**

Experimental data were shown as mean and standard deviation ( $X \pm SD$ ). The SPSS10 for Windows was used for statistical

analysis. The difference between each group was analyzed by  $t$  test. Significant difference was set at  $P < 0.05$ .

**RESULTS**

In this experiment, 476.5 nm, 488 nm, 496.5 nm, 514.5 nm, 532 nm, 808 nm wavelengths of laser radiation were respectively used for radiating the wall and ekstexine of the thin sample. Each datum was the mean of at least ten measurements of human normal small intestine tissue, and each wavelength of laser in the same way. Each time the sample was measured, the position of incident light spot on the sample was changed. The data had very good repetition. There were no significant differences in the diffuse reflectance and transmittance, the specular reflectance and collimated transmittance of the wall and ekstexine of the sample at each wavelength of laser radiation ( $P > 0.05$ ). Consequently, the measured results of the wall and ekstexine of the sample at the same wavelength of laser radiation were estimated by arithmetical average.

**Optical parameters of the tissue in Kubelka-Munk two-flux model**

The absorption coefficients, scattering coefficients, total attenuation coefficients and effective attenuation coefficients of human normal small intestine tissue in Kubelka-Munk two-flux model at 476.5 nm, 488 nm, 496.5 nm, 514.5 nm, 532 nm, 808 nm wavelengths of laser radiation are given in Table 1 and shown in Figure 4.

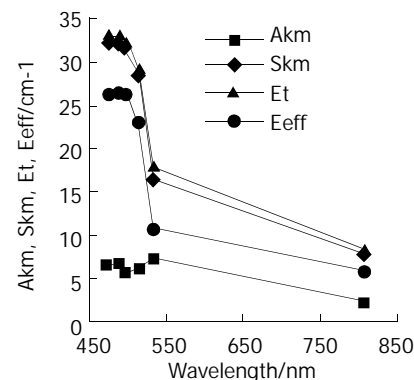


**Figure 4** Broken line graphs of  $A_{KM-\lambda}$ ,  $S_{KM-\lambda}$ ,  $E_t-\lambda$ ,  $S_{eff-\lambda}$  of human normal small intestine tissue.

**Table 1** The absorption coefficients, scattering coefficients, total attenuation coefficients and effective attenuation coefficients of human normal small intestine tissue in Kubelka-Munk two-flux model at six different wavelengths of laser irradiation

$\lambda/nm$	$A_{KM}/(cm^{-1})$	$S_{KM}/(cm^{-1})$	$E_t/(cm^{-1})$	$E_{eff}/(cm^{-1})$
476.5	26.3±1.15	6.67±0.32	33.0±1.09	32.3±1.53
488	26.5±1.19	6.47±0.29	33.0±1.09	32.3±1.53
496.5	26.4±1.18	5.82±0.24	32.2±1.05	31.7±1.49
514.5	23.2±1.12	6.06±0.28	29.3±0.97	28.6±1.37
532	10.8±0.52	7.27±0.37	18.0±0.89	16.5±0.81
808	5.92±0.26	2.29±0.14	8.21±0.40	7.89±0.39

**Light distribution of the tissue in Kubelka-Munk two-flux model along the tissue thickness**

Light distribution of  $i(x)$ ,  $j(x)$ ,  $I(x)$  of human normal small intestine tissue in Kubelka-Munk two-flux model that changed with tissue thickness at six different wavelengths of laser radiation are shown in Figure 5. Light distribution was automatically created by using the experimental data in Table 1 and Mathcad2001 for Windows.

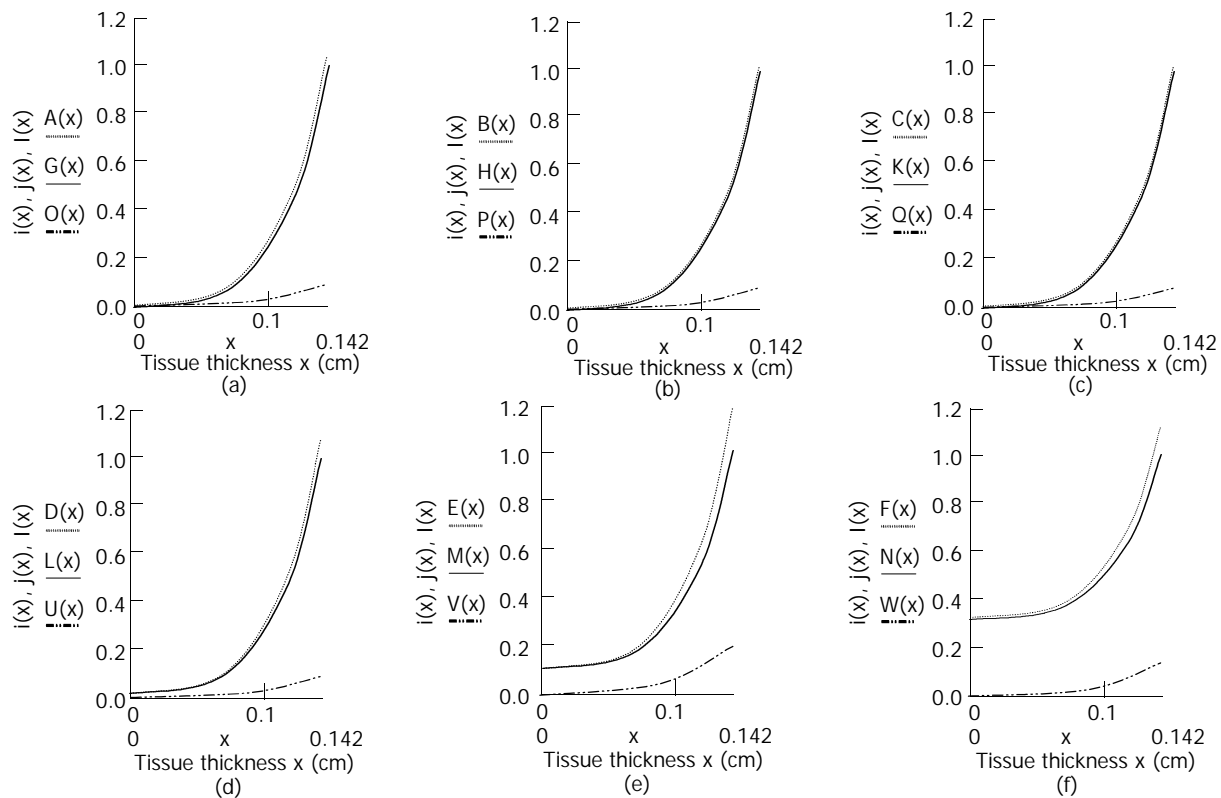


**Figure 5** Light distribution of  $i(x)$ ,  $j(x)$ ,  $I(x)$  of human normal small intestine tissue in Kubelka-Munk two-flux model changed with tissue thickness at six different wavelengths of laser radiation. (a)  $A(x)$ ,  $G(x)$  and  $O(x)$  respectively represented the forward and backward, and the total scattered photon fluxes of the tissue at 476.5 nm laser irradiation. (b)  $B(x)$ ,  $H(x)$  and  $P(x)$  respectively represented the forward, backward and the total scattered photon fluxes of the tissue at 488 nm laser irradiation. (c)  $C(x)$ ,  $K(x)$  and  $Q(x)$  respectively represented the forward, backward and the total scattered photon fluxes of the tissue at 496.5 nm laser irradiation. (d)  $D(x)$ ,  $L(x)$  and  $U(x)$  respectively represented the forward, backward and the total scattered photon fluxes of the tissue at 514.5 nm laser irradiation. (e)  $E(x)$ ,  $M(x)$  and  $V(x)$  respectively represented the forward, backward and the total scattered photon fluxes of the tissue at 532 nm laser irradiation. (f)  $F(x)$ ,  $N(x)$  and  $W(x)$  respectively represented the forward, backward and the total scattered photon fluxes of the tissue at 808 nm laser irradiation.

The results showed that there were differences both in optics properties of the tissue at six different wavelengths of laser radiation in Kubelka-Munk two-flux model, and in light distribution of  $i(x)$ ,  $j(x)$ ,  $I(x)$  of the tissue in Kubelka-Munk two-flux model which changed with the tissue thickness at six different wavelengths of laser radiation.

## DISCUSSION

Table 1 and Figure 4 show that there were no significant differences in the absorption coefficients of human normal small intestine tissue in Kubelka-Munk two-flux model at 476.5 nm, 488 nm, 496.5 nm laser radiation ( $P > 0.05$ ). The absorption coefficients of the tissue at 514.5 nm, 532 nm, 808 nm laser radiation obviously increased with decrease of these wavelengths. The scattering coefficients of the tissue at 476.5 nm, 488 nm, 496.5 nm laser radiation increased with decrease of these wavelengths. And the scattering coefficients of the tissue at 496.5 nm, 514.5 nm, 532 nm laser radiation obviously increased with increase of these wavelengths. The scattering coefficient of the tissue at 532 nm laser radiation was bigger than that of the tissue at 808 nm laser radiation. There were no significant differences in the total attenuation coefficients of the tissue at 476.5 nm and 488 nm laser radiation ( $P > 0.05$ ). The total attenuation coefficients of the tissue at 488 nm, 496.5 nm, 514.5 nm, 532 nm, 808 nm laser irradiation obviously increased with decrease of these wavelengths, and their effective attenuation coefficients revealed the same trend. It is suggested that the optical parameters of human tissues in Kubelka-Munk two-flux model can be measured by using the

measuring technology of light radiation, and the optical parameters of human tissues with pathological changes and normal human tissues can be compared and analyzed. The results provide a new method of information analysis for clinical diagnosis. Figure 5 shows there were no obvious differences in the forward, backward and the total scattered photon fluxes of the tissue at 476.5 nm, 488 nm, 496.5 nm laser irradiation. All of them obviously increased with attenuation of the tissue thickness. Attenuations of the forward, backward and the total scattered photon fluxes of the tissue at 514.5 nm laser radiation were slightly slower than those at 476.5 nm, 488 nm, 496.5 nm laser radiation. And attenuations of the forward, backward, and the total scattered photon fluxes of the tissue at 532 nm laser radiation were obviously slower than those at 476.5 nm, 488 nm, 496.5 nm, 514.5 nm laser radiation. Attenuations of the forward, backward, and the total scattered photon fluxes of the tissue at 808 nm laser radiation were all obviously slower than those at 476.5 nm, 488 nm, 496.5 nm, 514.5 nm, 532 nm laser radiation. Consequently light attenuation of human normal small intestine tissue at six different wavelengths of laser radiation increased with decrease of these wavelengths, and the change of light attenuation of the tissue accorded completely with the changing rule of penetrability of biological tissues at light radiation of different wavelengths, namely the penetrability of biological tissues from visible light to Infrared light, a range of wavelengths from 400 nm to 900 nm, increased with the increase of wavelengths. It was obvious that penetrability of biological tissues at 808 nm laser was better than the other five wavelengths of laser radiation. 808 nm laser may be used to treat the deep disease

focus in organisms by photodynamic therapy<sup>[29-32]</sup>. The results of measurement provide useful references and data to laser therapy that is used in clinics, and help improve the effectiveness of photodynamic therapy<sup>[33-35]</sup>.

## REFERENCES

- Feng L**, Wu YL, Zhu Q, Zhong J. Argon plasma coagulator in the endoscopic treatment of 78 patients with gastrointestinal polyps. *Shijie Huaren Xiaohua Zazhi* 2000; **8**: 1336-1338
- Cheng YS**, Shang KZ. Gastrointestinal imageology in China: a 50 year evolution. *Shijie Huaren Xiaohua Zazhi* 2000; **8**: 1225-1232
- Feng L**, Wu YL, Zhong J, Zhu Q. Argon plasma coagulation in the endoscopic treatment of verrucosal gastritis. *Shijie Huaren Xiaohua Zazhi* 2000; **8**: 1332-1335
- Li CZ**, Cheng LF, Gu Y, Wang ZQ, Yang YS, Liu QS, Linghu EQ. Obliteration effect of photodynamic therapy on small veins: an experimental study. *Zhongguo Jiguang Yixue Zazhi* 2003; **12**: 5-8
- Wan XQ**, Wang CP, Cheng K, Li LL, Xu SZ, Li CS, Yang ZQ. Study on the killing effect of in vitro photodynamic therapy using delta-aminolevulinic acid on HEP-2 cells. *Zhongguo Jiguang Yixue Zazhi* 2000; **9**: 102-104
- Chen WH**, Yu JX, Yao JZ, Shen WD, Liu JF, Xu DY. Pharmacokinetic studies on hematoporphyrin monomethyl ether: A new promising drug for photodynamic therapy of tumors. *Zhongguo Jiguang Yixue Zazhi* 2000; **9**: 105-108
- Liu FG**, Gu Y, Fu QT, Pan YM, Li JH. Absorptive characteristics of HMME and HpD in chicken comb skin and vascular endothelial cells. *Zhongguo Jiguang Yixue Zazhi* 2001; **10**: 9-12
- Ritz JP**, Roggan A, Isbert C, Müller G, Buhr HJ, Germer CT. Optical properties of native and coagulated porcine liver tissue between 400 and 2400nm. *Lasers Surg Med* 2001; **29**: 205-212
- Qu J**, MacAulay C, Lam S, Palcic B. Optical properties of normal and carcinomatous bronchial tissue. *Appl Opt* 1994; **33**: 7397-7405
- Liu G**, Xing D, Wang HM, Wu J. Study of protein in human gallstones by fourier transform infrared spectroscopy and surface-enhanced Raman spectroscopy. *Guangxue Xuebao* 2002; **22**: 441-446
- Sankaran V**, Everett MJ, Maitland DJ, Walsh JT Jr. Comparison of polarized-light propagation in biological tissue and phantoms. *Opt Lett* 1999; **24**: 1044-1046
- Kim AD**, Ishimaru A. Optical diffusion of continuous-wave, pulsed, and density waves in scattering media and comparisons with radiative transfer. *Appl Opt* 1998; **37**: 5313-5319
- Li J**, Li SR, Cao JB, Gao G. Laser-induced fluorescence spectrum of colon cancer *in vivo*. *Shijie Huaren Xiaohua Zazhi* 1999; **7**: 164-165
- Liao XH**, Chen ZL, Tang JM, Luo YS. An experimental study on optical properties of rat viscera. *Jiguang Zazhi* 2002; **23**: 74
- Li BH**, Xie SS, Lu ZK. Time-resolved spectroscopy for human esophageal and breast tissues *in vitro*. *Guangdianzi Jiguang* 2002; **13**: 1071-1073
- Gorti S**, Tone H, Imokawa G. Triangulation method for determining capillary blood flow and physical characteristics of the skin. *Appl Opt* 1999; **38**: 4914-4929
- Van der Putten WJM**, Van Gemert MJC. A modelling approach to the detection of subcutaneous tumours by haematoporphyrin-derivative fluorescence. *Phys Med Biol* 1983; **28**: 639-645
- Chen R**, Xie SS, Chen YI, Wang HP. Transmission properties of ray in blood in laser irradiation blood therapy. *Guangdianzi Jiguang* 2001; **12**: 1310-1312
- Wu GL**, Luo QM, Zeng SQ, Mu CP, Liu XD. Photon diffusion theory and its application in biomedicine. *Guangdianzi Jiguang* 2001; **12**: 323-328
- Cheng SY**, Huang JH, Lin WX, Zhang G, Huang XJ, Huang CH, Shen HY. Problems in measuring attenuation coefficient  $\mu_t$  of blood by direct measurement method. *Guangzi Xuebao* 2001; **30**: 1045-1049
- Liu XL**, Zhang R, Bao HJ, Zhong JK. Study on the method for determination of tissue optical properties by time resolved reflectance. *Shengwu Wuli Xuebao* 2001; **17**: 209-215
- Vogel A**, Dlugos C, Nuffer R, Birngruber R. Optical properties of human sclera, and their consequences for transscleral laser applications. *Lasers Surg Med* 1991; **11**: 331-340
- Graaff R**, Aarnoudse JG, De Mul FFM, Jentink HW. Light propagation parameters for anisotropically scattering media based on a rigorous solution of the transport equation. *Appl Opt* 1989; **28**: 2273-2279
- Wei HJ**, Li XY, Wu GY, Liu XX, Wei DJ, Tan RC. Scattering and absorbing characteristics of human arteries and veins in Kubelka-Munk model at He-Ne laser *in vitro*. *Zhongguo Jiguang* 2001; **A28**: 573-576
- Seiyama A**, Chen SS, Kosaka H, Shiga T. Microspectroscopic measurement of the optical properties of rat liver in the visible region. *J Microscopy* 1994; **175**: 84-89
- Pickering JW**, Prahl SA, Van Wieringen N, Beek JF, Sterenborg HJCM, Van Gemert MJC. Double-integrating-sphere system for measuring the optical properties of tissue. *Appl Opt* 1993; **32**: 399-410
- Zhu D**, Luo QM, Zeng SQ, Ruan Y. Changes in the optical properties of slowly heated human whole blood and albumen. *Guangxue Xuebao* 2002; **22**: 369-373
- Zhu D**, Luo QM, Zeng SQ, Yin M, Ruan Y. Modified double-integrating-sphere system for measuring the optical properties of tissue. *Guangzi Xuebao* 2001; **30**: 1175-1181
- Deng XH**, Gu Y, Huang F, Liu FG, Zhu JG, Pan YM. Preliminary study of cytotoxic effect of HMME mediated photodynamic action on synovial cells of rheumatoid arthritis *in vitro*. *Zhongguo Jiguang Yixue Zazhi* 2001; **10**: 218-222
- Liu FG**, Gu Y, Liu HL, Fu QT, Zhu JG, Pan YM, Li JH. An experimental study on the comparison of photodynamic effects of hematoporphyrin monomethyl ether and hematoporphyrin derivative. *Zhongguo Jiguang Yixue Zazhi* 2001; **10**: 69-73
- Gu Y**, Liu FG, Wang K, Zhu JG, Liang J, Pan YM, Li JH. A clinic analysis of 1216 cases of port wine stain treated by photodynamic therapy. *Zhongguo Jiguang Yixue Zazhi* 2001; **10**: 86-89
- Zeng CY**, Huang P, Yang D, Yang SM, Chen F. A study on liver damage induced by photodynamic therapy. *Zhongguo Jiguang Yixue Zazhi* 2000; **9**: 141-145
- Zeng CY**, Yang D, Huang P, Zhang HJ, Chen J, Lu GR. Long-term follow-up results of 70 liver cancer cases received ultrasound guided percutaneous PDT. *Zhongguo Jiguang Yixue Zazhi* 2000; **9**: 146-149
- Tao R**, Gu Y, Liu FG, Zeng J, Zhang L, Pan YM. Mechanism of photosensitized reaction induced by hematoporphyrin monomethyl ether *in vitro*. *Zhongguo Jiguang Yixue Zazhi* 2002; **11**: 149-153
- Zhou SR**, Liu CY, Xu SZ, Xiong LY, Zhou XF.  $\delta$ -ALA-PDT in treatment in BXSb lupus-prone mice: An experimental study. *Zhongguo Jiguang Yixue Zazhi* 2002; **11**: 154-156

Edited by Zhu LH and Wang XL